Materials Research Innovations

ISSN: 1432-8917 (Print) 1433-075X (Online) Journal homepage: https://www.tandfonline.com/loi/ymri20

Effect of annealing on the structural, morphological, optical and electrical properties of Al-Zn co-doped SnO_2 thin films

K. Pakiyaraj, V. Kirthika & K. Karthik

To cite this article: K. Pakiyaraj, V. Kirthika & K. Karthik (2019): Effect of annealing on the structural, morphological, optical and electrical properties of Al-Zn co-doped SnO_2 thin films, Materials Research Innovations, DOI: 10.1080/14328917.2019.1628498

To link to this article: https://doi.org/10.1080/14328917.2019.1628498

Published online: 10 Jun 2019.

MATERIALS RESEARCH INNOVATIONS
https://doi.org/10.1080/14328917.2019.1628498

Taylor & Francis
Taylor & Francis Group

Effect of annealing on the structural, morphological, optical and electrical properties of Al-Zn co-doped SnO_2 thin films

K. Pakiyaraj[a], V. Kirthika[b] and K. Karthik[c]

[a]Department of Physics, Arulmigu Palaniandavar College of Arts & Culture, Palani, India; [b]Department of Physics, St. Antonys's College of Arts and Sciences for Women, Dindigul, India; [c]Department of Physics, Bharathidasan University, Tiruchirappalli, India

ABSTRACT

Aluminum–Zinc co-doped SnO_2 thin films were successfully synthesised onto glass substrates by spray-pyrolysis processing. The structural, morphological, optical and electrical properties of co-doped thin films as deposited at 400°C, 500°C, and 600°C and were studied using various techniques. The XRD results show the films possessed polycrystalline SnO_2 with tetragonal rutile structure. The average crystallite size found to be 39 (pure) and 31 nm (co-doped). AFM images showed the annealing temperature effects surface morphology of the films. The transmittance of thin films is up to 80 to 85% in the visible region. The bandgap of the films has been calculated for different annealing temperature and they lie within the range of 3.87 – 4.21 eV. Electrical properties of co-doped thin films were studied through Hall measurement. Furthermore, the prepared co-doped thin films will be useful in optoelectronics and gas sensing applications.

ARTICLE HISTORY
Received 17 April 2019
Accepted 1 June 2019

KEYWORDS
Spray pyrolysis; XRD; SEM with EDAX; AFM; Optical and electrical properties

Introduction

Tin oxide thin films have been attracting interest in its applications on liquid gas sensors solar cells and liquid crystals displays, etc., may methods such as CVD [1], Spray Pyrolysis [2], Sputtering [3], molecular beam epitaxy [4] and spin coating [5] has been used to produce thin films. The spray pyrolysis process has some advantage over the other techniques due to excellent compositional control homogeneity at the molecular level due to the mixing of liquids precursors and lower crystallisation temperature. At the same time, the spray pyrolysis of methods offers the possibility of preparing a small well as large area coating of its Aluminium–Zinc co-doped SnO_2 (AZSO) thin films at low cost for technological applications [5–7]. Co-doping with solute atoms is an effective method to improve various properties of TCO, films [8] Gopinadhan et al. [9] have reported the co-doped SnO_2 films deposited by spray pyrolysis and have high conductivity and good optical transmittance in the visible regions. SnO_2 thin films are very useful in wastewater treatment, optoelectronics, gas sensing and biological applications [10–25]. But, few researchers on sol-gel pyrolysis derived Co-doped SnO_2 films were reported. In this work, co-doped SnO_2 thin films were coated into glass substrate using spray pyrolysis. Structural, morphological optical and electrical properties are characterised. In this paper, the deposition and the characterisation of doped SnO_2 thin films. Hence, the effect on the annealing temperature of structural, morphological and optical properties of Al-Zn-SnO_2 thin films has been discussed.

2. Experimental details

Pure and Al, Zn doped SnO_2 thin films were deposited glass substrate by the spray pyrolysis technique. As a starting material and dopant source $SnCl_4$. $5H_2O$, $AlCl_3.5H_2O$, and $ZnCl_2$. $6H_2O$ were used as a precursor and doping precursor was dissolved in ethanol and stirred 4 h at 50°C. The starting stoichiometry concentration of the pure and co-doped solution was 4% in the solution. Firstly pure and Al-Zn doped SnO_2 layers were sprayed on glass substrates at 400°C. The substrate mounted on a hot plate that hot plate connected to dimmastrate and high sensitive digital thermometer for maintaining hot plate at 400°C. The spray rate and substrate to nozzle distance were maintained at 10 mL/min and 25 cm, respectively. Then, prepared samples were annealed at 500°C and 600°C by muffle furnace.

2.1 Characterisation

The crystalline structure was carried out by a Rigaku X-ray diffractometer model DmAX 2200 with a copper anti-cathode (CuK_α,λ = 1.5Å) with an angle range (2θ) of 20–70°. The surface morphology of the films and the cross section films thickness were studied by field emission scanning electron microscope (FESEM). AFM images were obtained by using a multimode scanning probe microscope with nanoscopic instruments and confirmation of doping material by EDAX. The optical parameters were measured using a Shima DZU-UV-3101PC bandgap (Eg) was evaluated from a plot of $(ah\nu)^2$ versus hν photon energy.

3. Results and discussion

3.1 Structural properties

The X-ray diffractogram of the pure SnO_2 thin film prepared at the substrate temperature of T_s = 400°C and annealed at 500°C and 600°C are shown in Figure 1–3. The XRD pattern shows the preferred orientation at 2θ = 37.94° with the plane (2 0 0) confirmed the presence of SnO_2 with the tetragonal crystal structure as well as the observed other characteristics peaks with the planes corresponding to (1 1 0), (2 1 1) are well-

CONTACT K. Pakiyaraj kpakiyaraj@gmail.com Department of Physics, Arulmigu Palaniandavar College of Arts & Culture, Palani 624 601, India

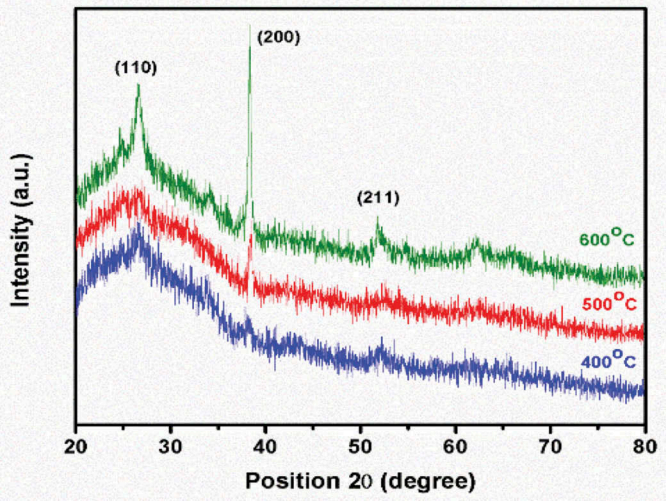

Figure 1. XRD pattern of pure SnO_2 thin films prepared at 400°C, annealed at 500°C and 600°C.

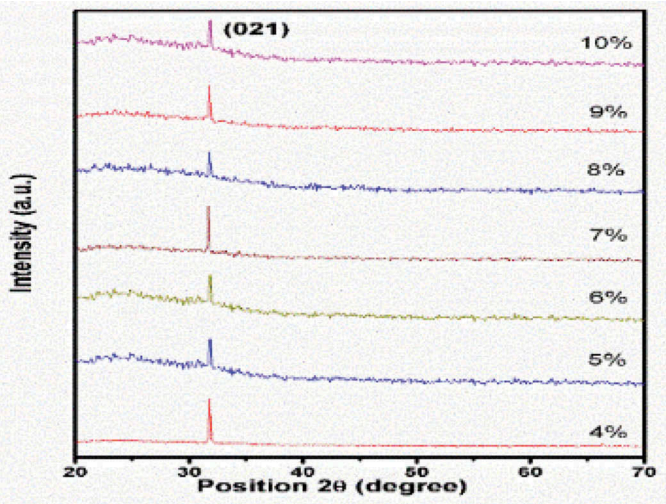

Figure 2. XRD pattern of the Al -Zn co-doped SnO_2 (4%, 5%, 6%, 7%, 8%, 9% and 10%) thin films .annealed at 500°C.

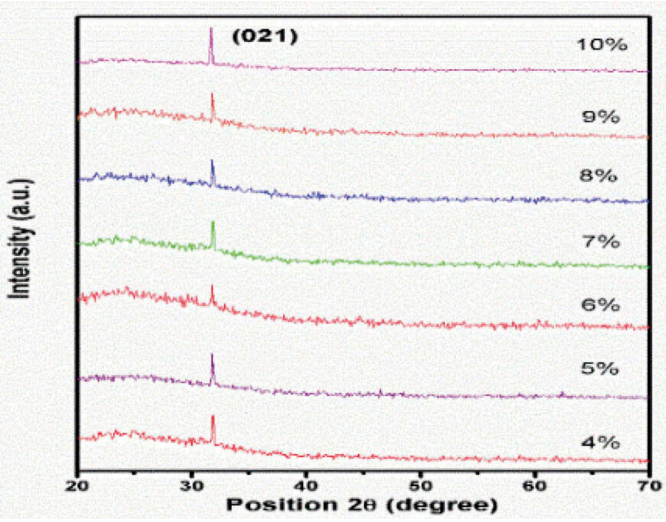

Figure 3. XRD pattern of the Al – Zn Co-doped SnO_2 (4%, 5%, 6%, 7%, 8%, 9% and 10%) thin films.annealed at 600°C.

matched with standard JCPDS File No.46–1088. The appearance of characteristic peaks at different positions revealed that the thin films are in polycrystalline nature. It can be noticed

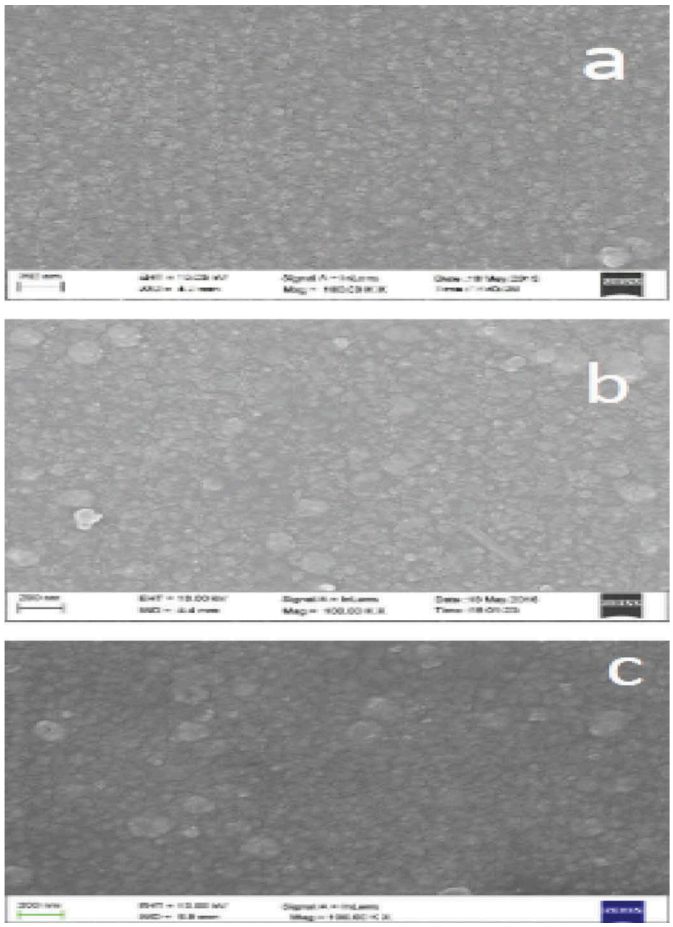

Figure 4. FESEM micrograph of pure SnO_2 thin film prepared at 400°C annealed at 500°C 600°C.

that the intensity of the peak corresponding to (2 0 0) is increased upon the increase of temperature which implies the crystallisation of the films. Furthermore, there are no any other additional peaks which are irrelevant to SnO_2. This result is indicating the purity of the prepared thin films. The Crystallite size of the prepared thin films was estimated using the following Scherer's Formula [26,27].

$$D = k\lambda/\beta\cos\theta \quad (1)$$

where D is the crystallite size, K is a constant and its value is 0.9, λ is a wavelength of X-Ray beam used for diffraction, β is the full width at half maxima and θ is the Diffraction angle. The crystallite size of the prepared thin films was estimated to be 48, 8, 16 nm for 400°C, 500°C, and 600°C respectively. Hence, the prepared thin films are justified to be nanocrystalline and also the mean crystallite size decreased with respect to annealing temperature. This annealing temperature affects the crystallinity of the thin films.

3.2 FESEM with EDAX analysis

Figure 4 shows FESEM images of pure SnO_2 thin films prepared at the substrate temperature T_S = 400°C and annealed at 500°C, 600°C, respectively. It can be clearly seen from the FESEM images that the thin films have been formed with dense, crack-free and smooth nature. It is observed from FESEM images that the spherical-shaped particles changed to square shape upon the increase of temperature on the surface morphology. This is possible due to the change in kinetics

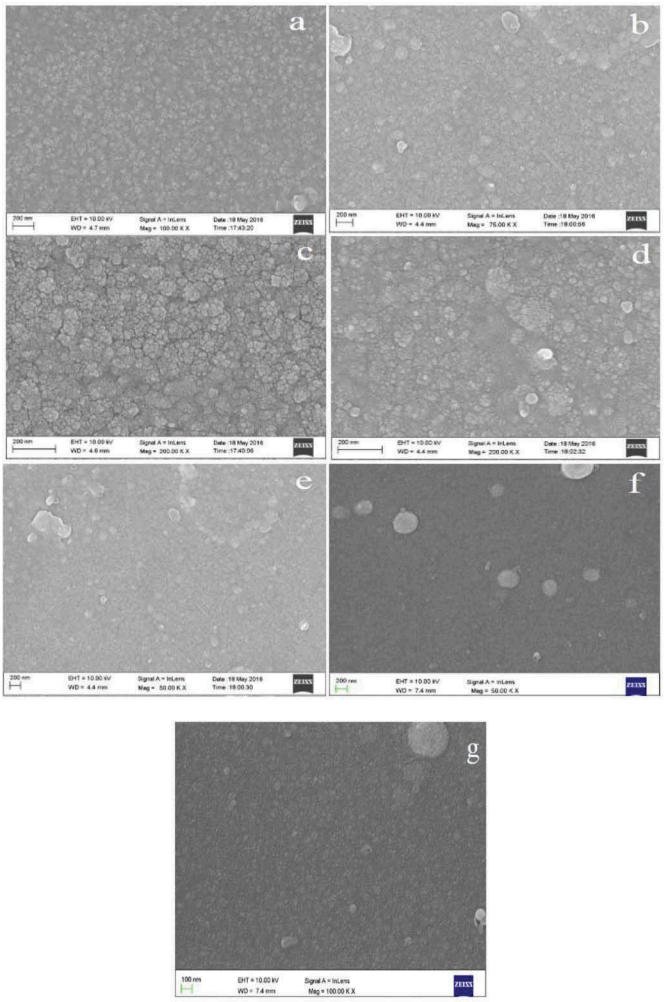

Figure 5. FESEM micrographs of the Al – Zn codoped SnO_2 thin films (a to g (a = 4%, = 5%,c = 6%,d = 7%,e = 8%,f = 9%, g = 10%)) annealed at 500°C.

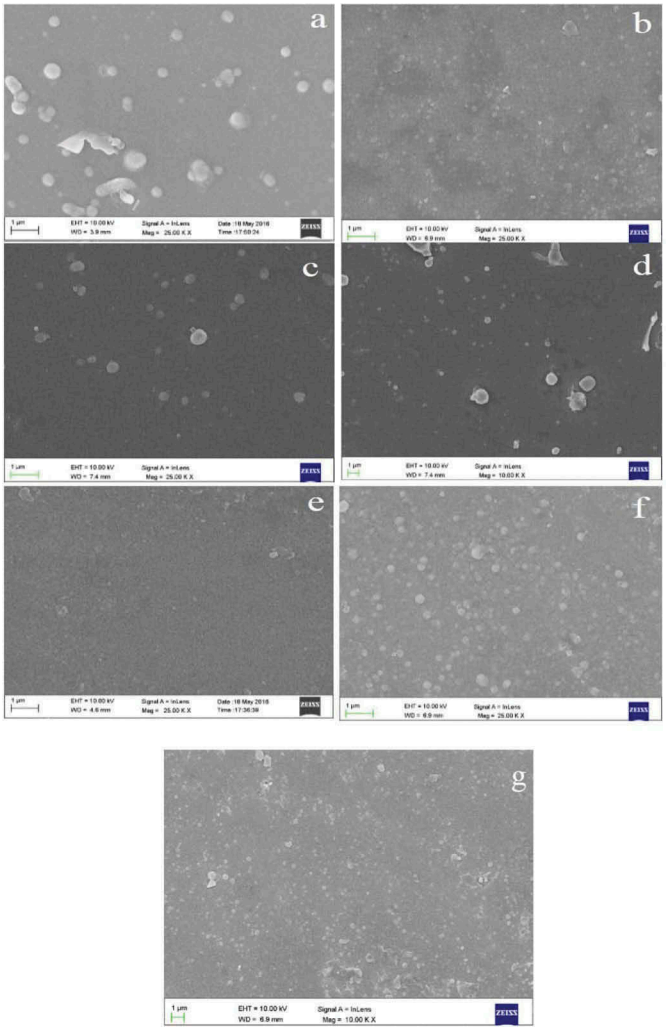

Figure 6. FESEM micrographs of the Al – Zn codoped SnO_2 thin films (a to g (a = 4%, = 5%,c = 6%,d = 7%,e = 8%,f = 9%, g = 10%)) annealed at 600°C.

during heat treatment. Furthermore, the morphology was ascertained by FESEM analysis. FESEM images showed the clear, crack-free, dense and smooth morphology of the prepared thin films with the presence of nanoparticles. FESEM images are apparently showed the increase of particle size upon the increase of temperature. This is due to the grain growth as a consequence agglomeration of particles can take place. Hence, the resultant particle size was found to be higher for the films subjected to 600°C. The impact of Al and Zn Co-doping on the surface morphology of SnO_2 is examined by FESEM analysis. Figures 5&6 show FESEM images of the prepared thin films show the smooth, dense, crack-free surface. The homogeneous deposition of thin films with fine and granular nanoparticles can be viewed through FESEM images. It is apparently seen that particle size is decreasing upon the increase of doping but at the same time from the 9% doping onwards the particle size tends to increase again. Also, increasing the annealing temperature causes the increase of particle size which is due to the grain growth thereby agglomeration took place and resulted in the increase of particle size. The approximate particle size was measured from the FESEM images and it lies in the range between 20 and 30 nm. The EDAX Spectra of the prepared SnO_2 thin films showed an appropriate peak belongs to the elements Sn and O only. This is confirmed the purity of films free from any other contaminants (Table 1–3). The peak at around 2KeV emerged from the substrate EDAX spectra (Figure7-9) substantiated of Al, Zn, Sn and O elements in the prepared thin films. The other peaks are appeared due to the substrate.

Table 1. Elemental composition of Al-Zn Co-doped SnO_2 (Wt.10%) at 400°C.

Elements	Weight Percentage (%)	Atomic Percentage (%)
Sn	98.00	95.44
Al	0.41	1.75
Zn	1.59	2.81

Table 2. Elemental composition of Al-Zn Co-doped SnO2 (Wt.10%) at 500°C.

	Weight Percentage (%)	Atomic Percentage (%)
Sn	95.87	89.07
Al	2.12	7.58
Zn	2.01	3.35

Table 3. Elemental composition of Al-Zn Co-doped SnO2 (Wt.10%) at 600°C.

Elements	Weight Percentage (%)	Atomic Percentage (%)
Sn	97.00	95.44
Al	1.41	2.95
Zn	**1.59**	**2.61**

3.3 AFM analysis

AFM images of AZSO thin films prepared at the substrate temperature of 400°C and annealed at 500°C and 600°C are shown in Figure10. The as-prepared thin film at T_s = 400°C shows the growth of crystallites from the inner towards the top of the surface and it seems like nanotips. This may be due to the evaporation of by-products during the spraying and resulted in the formation of the tip like topography. But after the annealing at 500°C, the length of the tips seems to decrease. Finally, increasing annealing temperature led to the agglomeration. The root-mean-square roughness (RMS) values of the film determined using the relation [28]. The average crystallite size was estimated from the 2D image view and it is about 25 nm.

3.4 Optical properties

The fundamental absorption corresponding to the optical transition of the electrons from the valence band to the conduction band can be used to determine the nature and

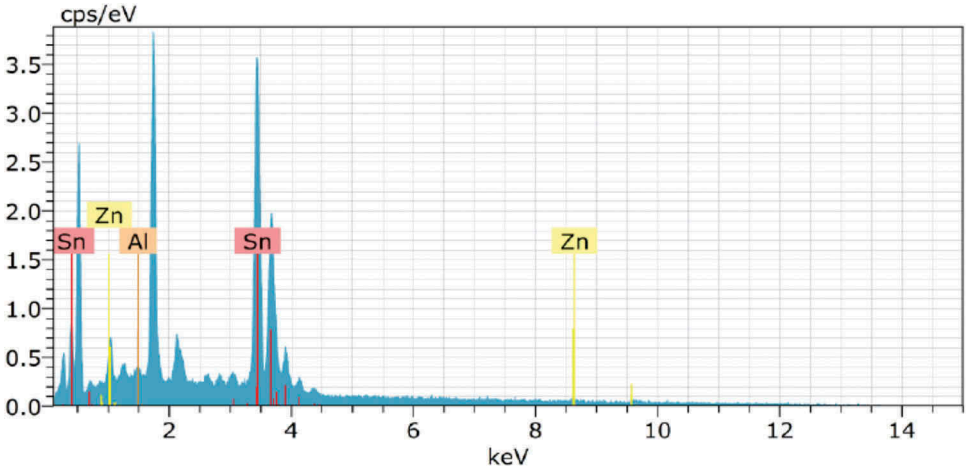

Figure 7. EDAX spectrum of the Al-Zn Co-doped SnO2 thin film (Wt.10%) prepared at 400°C.

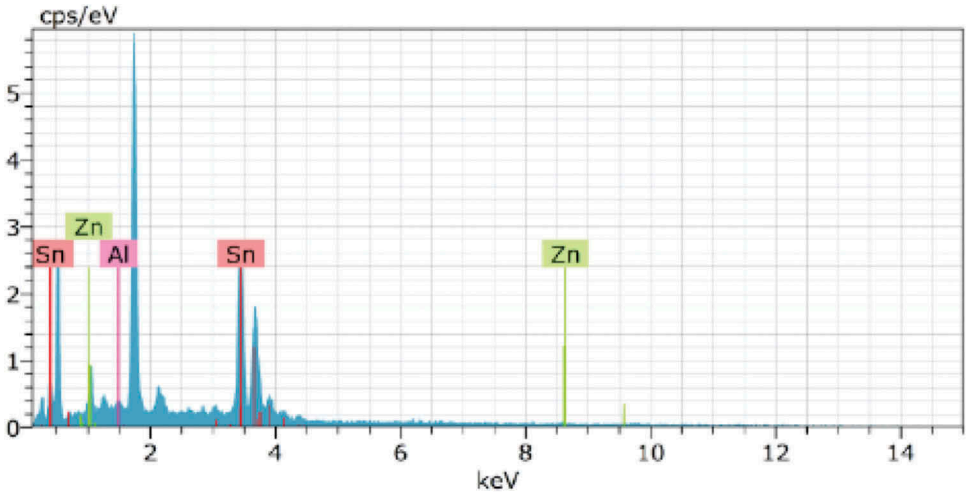

Figure 8. EDAX spectrum of the Al – Zn Co-doped SnO2 thin film (Wt.10%) annealed at 500°C.

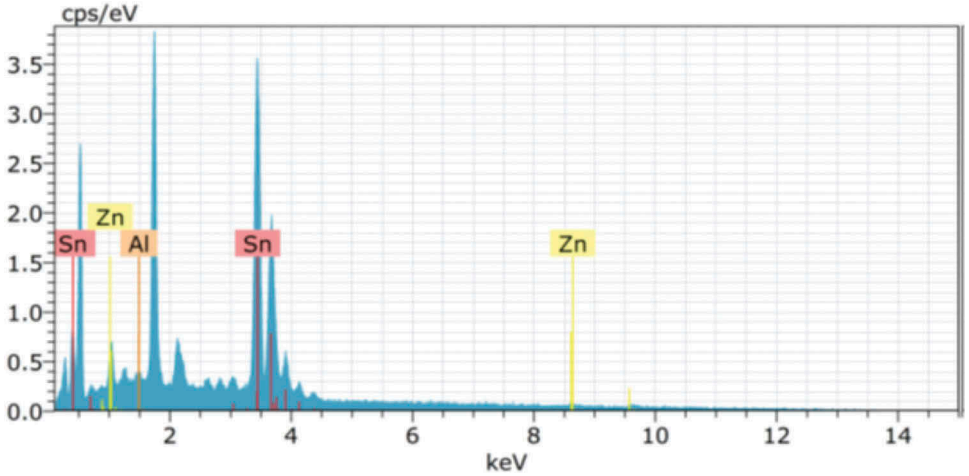

Figure 9. EDAX spectrum of the Al – Zn Co-doped SnO2 thin film (Wt.10%) annealed temperature at 600°C.

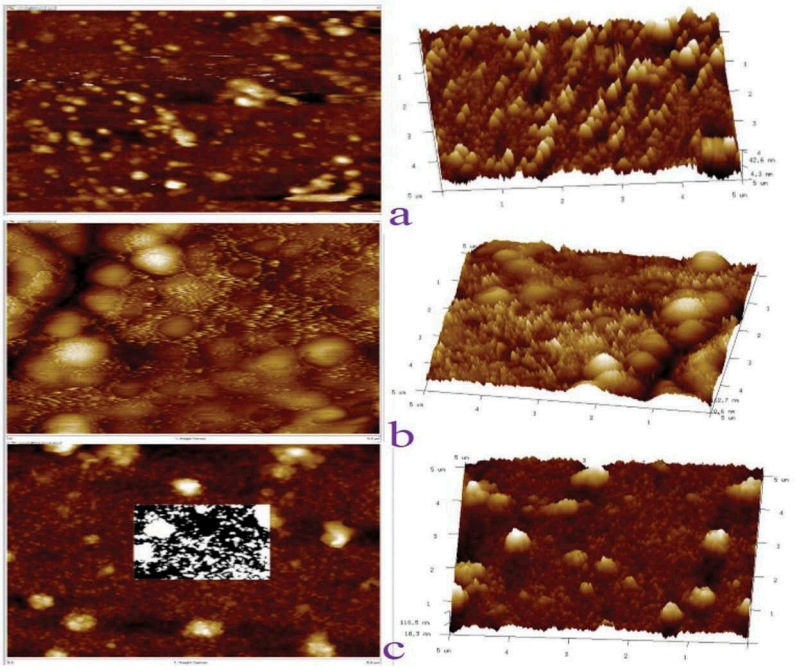

Figure 10. 2 and 3 dimensional atomic force micrographs for Al-Zn co-doped SnO_2 thin films prepared at 400°C, annealed at 500°C and 600°C (10 Wt.%).

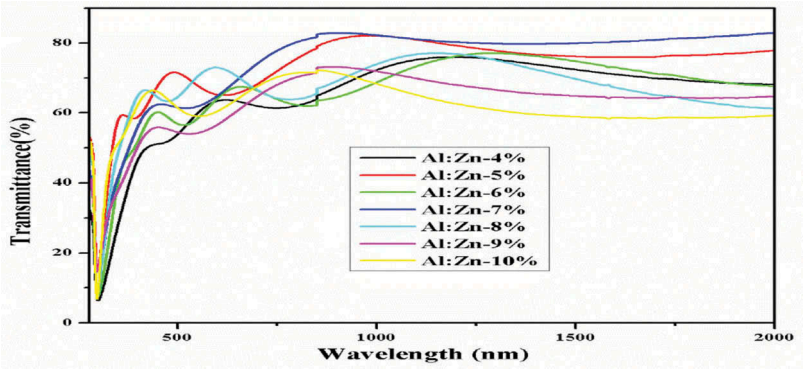

Figure 11. Optical transmittance spectra of Al-Zn-SnO_2 (4%,5%,6%,7%,8%,9% and 10%) thin films deposited on glass substrates prepared at 400°C.

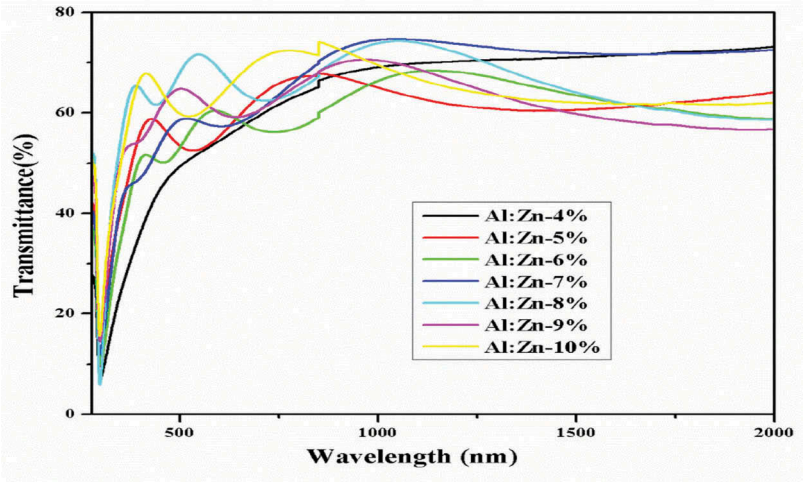

Figure 12. Optical transmittance spectra of Al-Zn -SnO_2 (4%,5%,6%,7%,8%,9% and 10%) thin films annealed at 500°C.

values of the bandgap (Eg) of the films. Depending on the characteristic property of the material, different theoretical equations have been used to calculate the absorption coefficient (α) value as a function of photon energy (hν). In this case, the films are polycrystalline, the (αhν) curves correspond to crystalline material with direct-allowed transitions (direct bandgap) can be used to calculate the bandgap by classical relation as given below [28].

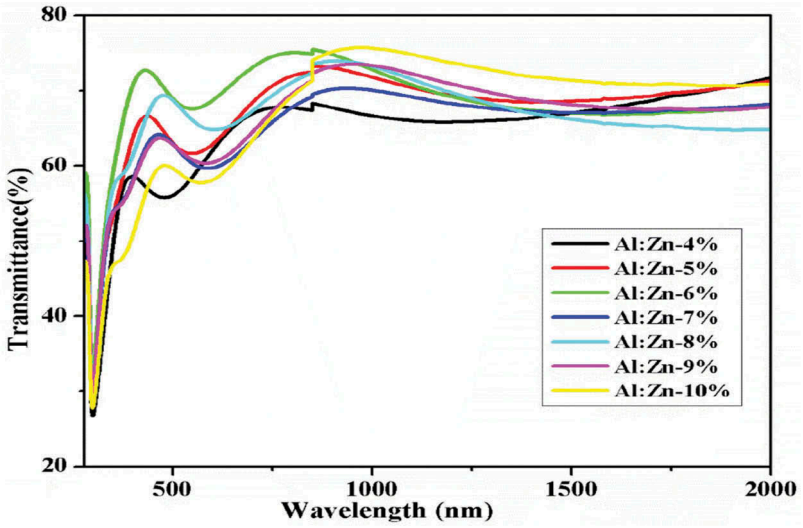

Figure 13. Optical transmittance spectra of Al-Zn-SnO_2 (4%,5%,6%,7%,8%,9% and 10%) thin films annealed at 600°C.

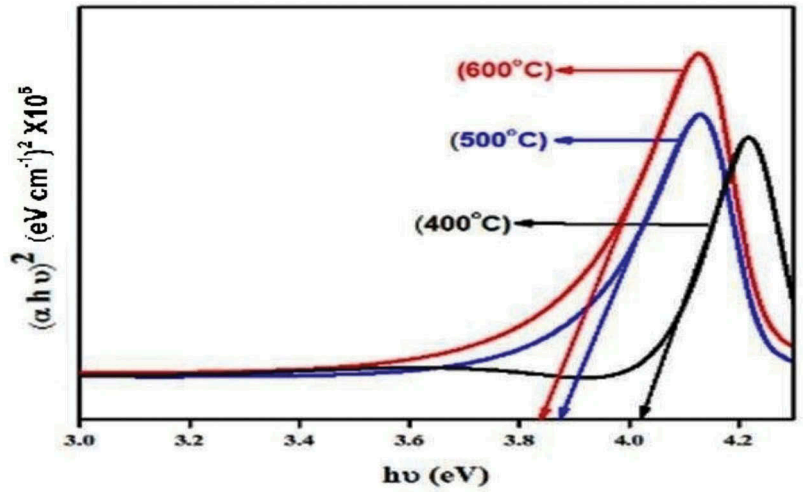

Figure 14. Bandgap of pure SnO_2 thin films at 400°C, 500°C and 600°C.

$$\alpha h\nu = A\left(h\nu - E_g\right)^n \quad (2)$$

where E_g is the optical band gap. A is a constant and the exponent 'n' depends on the transition [29]. The UV-Vis transmittance spectra of SnO_2 thin films deposited on a glass substrate at the prepared substrate temperature of 400°C and annealed temperature of 500°C, 600°C are shown in Figure 11–13. The transmittance spectra revealed that the films are highly transparent in the visible region with the transparency of 85%, 95% and 70% for 400°C, 500°C and 600°C annealed SnO_2 thin films, respectively. An increase of annealing temperature to 500°C led to the enhancement of transparency, but further increasing the annealing temperature (600°C) decreased the transparency of films, which may be caused by the increase of the density due to higher temperature effects. The absorption edge is shifted from lower wavelength region to higher wavelength region (i.e. red shifted) is an indication of a decrease of the band gap of the SnO_2 thin films upon increasing annealing temperature. Considering direct band transition in SnO_2 thin film, a plot between $(\alpha h\upsilon)^2$ versus photon energy (hυ) has been drawn and which is shown in Figure 14. Extrapolation of the linear region of these plots to $(\alpha h\upsilon)^2$ gives corresponding direct energy bandgap. The band gap values of 4.02 eV, 3.88 eV, and 3.84 eV have been obtained for the SnO_2 thin films prepared at 400°C and annealed at 500°C and 600°C, respectively. The obtained

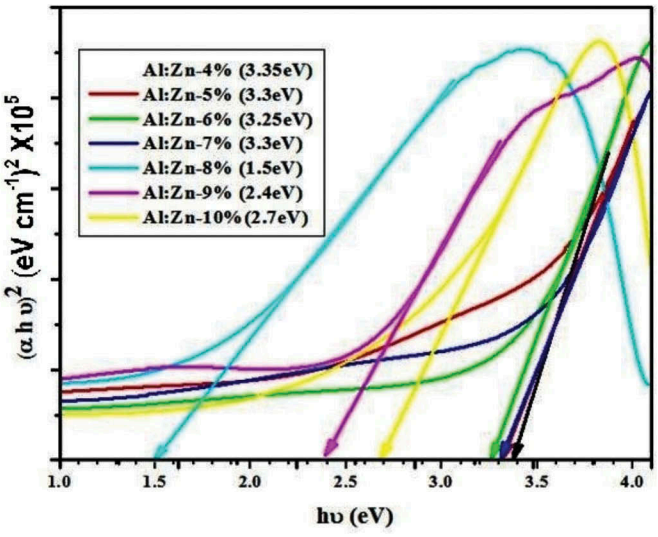

Figure 15. Bandgap of Al-Zn- SnO_2 (4%,5%,6%,7%,8%,9% and 10%) thin films annealed at 500°C.

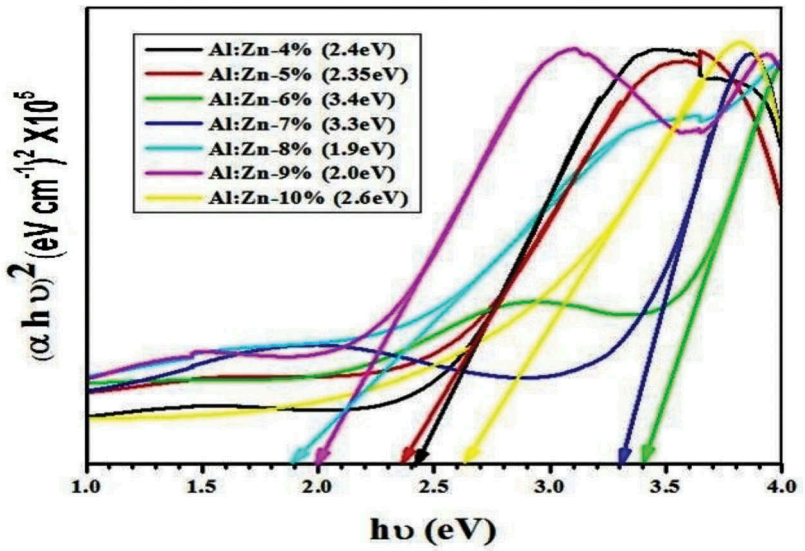

Figure 16. Bandgap of Al-Zn-SnO_2 (4%,5%,6%,7%,8%,9% and 10%) thin annealed at 600°C.

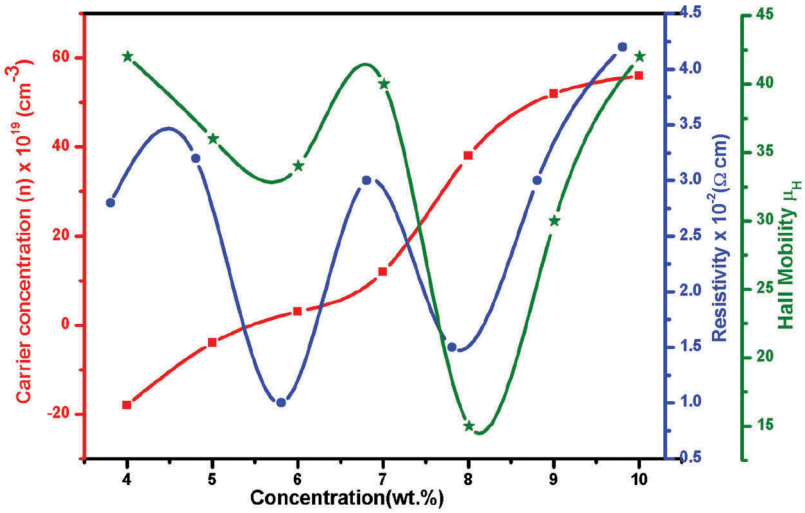

Figure 17. Plot for carrier concentration, Hall mobility, Resistivity Vs Al-Zn Co-doped SnO2 thin film annealed at 500°C.

bandgap values are in good consistent with the literature [30,31].

The UV-Vis transmittance spectra of Al and Zn co-doped SnO_2 thin films prepared temperatures at T_s = 400°C and annealed temperature at 500°C and 600°C are shown in Figures. All the films have transparency of around 80%. It can be seen that in all the thin films the appearance of UV radiation with Al and Zn doped SnO_2. Figures (14–16) show the Tauc's plot of $(\alpha h\upsilon)^2$ vs photon energy hυ(eV). From these Tauc's plot bandgap energy of the thin films was to be (2.35 to 3.55eV), (2.5 to 3.55eV) and (1.5 to 3.35eV) for 400°C, 500°C, and 600°C respectively. Increasing the annealing temperature leads to a decrease in bandgap energy values.

3.5 Electrical properties

Figure 17 shows the Plot for carrier concentration, Hall mobility, the resistivity of AZSO thin films grown on glass substrate annealed at 500°C. It is found that hall mobility strongly depends on the carrier density. Hall mobility increased with increasing the carrier density which is interesting behaviour. The interesting relation between hall mobility and the carrier density in the AZSO films has been reported in other oxides.

It is important to investigate the temperature dependents of the conductivity hall mobility, resistivity and its carrier density to reveal the transport mechanism. AZSO films showed relativity highly hall mobility. Hall mobility and carrier density randomly increasing and decreasing depending upon the temperature. Whatever the measurement temperature we have clearly noticed mobility and the carrier concentration depends on the annealing temperature. As a result, prepared thin films are inappropriate for two materials because of their low conductivity. However, it was found that the conductivity and free carrier density can be controlled in a wide range by changing the Al, Zn concentration and temperature [32–41]. At higher concentration of Wt.10% the hall mobility of AZSO thin films increasing the annealed temperature of 500°C. So this condition to make the film is suitable for gas sensing applications.

4. Conclusion

Al and Zn doped SnO_2 nanocrystalline thin films have been successfully prepared on the glass substrate by spray pyrolysis

method. It was found that the nanocrystalline SnO_2 grains possess structure features of the tetragonal rutile structure. The crystallite size was calculated using Scherrer's formula and it was in the range of 30 to 35 nm. The thickness of the thin films was measured and it was about 1.75 μm to 1.05 μm 400°C to 600°C, respectively. FESEM images demonstrated the fine and granular nanoparticles in the size range of 20 to 30 nm. EDAX spectra confirmed the presence of Al, Zn, Sn and O elements. The prepared thin films have shown higher transparency (80% to 85%) in the visible region. Hall mobility was observed to be monotonically increased with the increase of Al and Zn content in SnO_2 thin films. However, it was found that the conductivity and free carrier density can be controlled in a wide range by changing the Al and Zn concentration. Therefore, it is clear that Al-Zn codoped SnO_2 thin film is a promising candidate for optoelectronics and gas sensors applications.

Disclosure statement

No potential conflict of interest was reported by the authors.

Notes on contributors

Dr. K. Pakiyaraj is currently working as an Assistant Professor in the Department of Physics, Arulmigu Palaniandavar College of Arts and Culture, Palani – 624 601, India. His field of the research includes Nanostructured materials and thin films for energy, optoelectronic and gas sensing applications.

V. Kirthika is currently working as an Assistant Professor in the Department of Physics, St. Antony's College of Arts and Sciences for Women, Dindigul – 624 005. Her field of research Nanostructured thin films for optoelectronics and gas sensing applications.

Dr. K. Karthik did Ph. D work on "Photocatalytic and Biological Studies of Metal Oxide Nanoparticles and Nanocomposites". He has published more than 25 research articles in reputed journals. He has total citations: 271, h-index: 11, i-10 index: 11 (From Google scholar citations: https://scholar.google.co.in/citations?user=hU-0UQsAAAAJ&hl=en). He is a very active member in ResearchGate and his RG score: 63.15, Total Research Interest: 1069.0, Recommendations: 13,965, Reads: 58,372 (From Research Gate: https://www.researchgate.net/profile/K_Karthik7). He has participated in more than 25 international and national conferences. His field of research includes crystal growth, semiconductors nanostructured materials, nanomaterials, biomaterials, thin films, bimetallic and trimetallic nanocomposite materials for energy, environmental and biological applications. He is the active reviewer for various reputed journals.

Statement of Novelty

- Aluminium–Zinc Co-doped SnO_2 nanocrystalline thin films were prepared by spray pyrolysis method.
- Al-Zn-Co doped SnO_2 thin films were deposited by different annealing temperatures (400°C, 500°C and 600°C).
- Structural, optical and electrical properties of AZSO thin films as deposited (400°C, 500°C and 600°C) were characterised using various techniques.

References

[1] Musat V, Texeira B, Fortunato E, et al. Al-doped ZnO thin films by sol–gel method. Surf Coat Technol. 2004;180:659.

[2] Ri KH, Wang Y, Zhou WL, et al. The structural properties of Al doped ZnO films depending on the thickness and their effect on the electrical properties. Appl Surf Sci. 2011;258:1283.

[3] Cusunova JR, Heredia EABojorge CD, et al. Structural characterization of supported nanocrystalline zno thin films prepared by dip-coating. Appl Surf Sci. 2011;257:10045.

[4] Chowdhury I, Blaine TGougam AB. Optical transmission enhancement of fluorine doped tin oxide (fto) on glass for thin film photovoltaic applications. Energy Procedia. 2013;42:660. DOI: 10.1016/j.egypro.2013.11.068

[5] Ahmed SF, Khan SGhosh PK, et al. Effect of al doping on the conductivity type inversion and electro-optical properties of sno2thin films synthesized by sol-gel technique. J Sol-gel Sci Technol. 2006;39:241.

[6] Vijayalakshmi S, Venkataraj SSubramanian M, et al. Physical properties of zinc doped tin oxide films prepared by spray pyrolysis technique. J Phys D: Appl Phys. 2008;41:035505.

[7] Moharrami F, Bagheri Mohagheghi MAzimi-Juybari H, et al. Structural, electrical, optical, thermo electrical and photoconductivity properties of the sno2–al2o3 binary transparent conducting films deposited by the spray pyrolysis method. Phys Scr. 2012;85(6):015703.

[8] Abdullah N, Ismail NMNuruzzaman DM. Preparation of tin oxide (sno2) thin films using thermal oxidation. Iop Conference Series: Materials Science and Engineering. 2018;319:01022. DOI: 10.1088/1757-899X/319/1/012022

[9] Smith A, Laurent JMSmith DS, et al. Relation between solution chemistry and morphology of sno2-based thin films deposited by a pyrosol process. Thin Solid Films. 1995;266:20.

[10] Heidari MR, Varma RS, Ahmadian M, et al. Photo-fenton like catalyst system: activated carbon/CoFe2O4 nanocomposite for reactive dye removal from textile wastewater. Appl Sci. 2019;9:963.

[11] Malakootian M, Gharaghani MA, Dehdarirad A, et al. ZnO nanoparticles immobilized on the surface of stones to study the removal efficiency of 4-nitroaniline by the hybrid advanced oxidation process (UV/ZnO/O3). J Mol Struct. 2019;1176:766.

[12] Hq A, Pourseyedi S, Mt M, et al. Green synthesis of zinc sulfide (ZnS) nanoparticles using Stevia rebaudiana Bertoni and evaluation of its cytotoxic properties. J Mol Struct. 2019;1175:214.

[13] Prabukanthana P, Lakshmia R, Harichandran G, et al. Photovoltaic device performance of pure, manganese (Mn2+) doped and irradiated CuIn Se2 thin films. New J Chem. 2018;42:11642–11652.

[14] Rajesh Kumar T, Prabukanthan PHarichandran G. Comparative study of structural, optical and electrical properties of electrochemically deposited eu, sm and gd doped znse thin films. J Mater Sci: Mater Electron. 2018;29:5638.

[15] Rajesh Kumar T, Prabukanthan P, Harichandran G, et al. Physicochemical and electrochemical properties of Gd3 +-doped ZnSe thin films fabricated by single-step electrochemical deposition process. J Solid State Electrochem. 2018;22:1197.

[16] Francis PDhanuskodi S, et al. High performance supercapacitor behavior of hydrothermally synthesized cdte nanorods. J Mater Sci: Mater Electron. 2018;29:17397.

[17] K, Vijayalakshmi SAnukorn Phuruangrat V, et al Multifunctional Applications of Microwave-Assisted Biogenic TiO2 Nanoparticles. J Clust Sci. 2019. DOI: doi:10.1007/s10876-019-01556-1

[18] Karthik K. Microwave assisted cdo–zno–mgo nanocomposite and its photocatalytic and antibacterial studies. J Mater Sci: Mater Electron. 2018;29:18519–18530.

[19] Malakootian M, Ehrampoush MH, Mahdizadeh H, et al. Comparison studies of raw and oxidized multi-walled carbon nanotubes H2SO4/HNO3 to remove p-nitroaniline from aqueous solution. J Water Chem Technol. 2018;40:327.

[20] Malakootian M, Mahdizadeh H, Dehdarirad A, et al. Photocatalytic ozonation degradtion of ciprofloxacin using ZnO nanoparticles immobilized on the surface of stones. J Dispers Sci Technol. 2019;40(6):846–854.

[21] HakimehMahdizadeh M. Process safety and environmental protection. 2019;123:299.

[22] Karthik K, Dhanuskodi S, Gobinath C, et al. Ultrasonic-assisted CdO–mgO nanocomposite for multifunctional applications. Mater Technol. 2019;34(7):403.

[23] Karthik K, Dhanuskodi S, Gobinath C, et al. Multifunctional properties of CdO nanostructures Synthesised through

microwave assisted hydrothermal method. Mater Res Innovations. 2018. DOI:10.1080/14328917.2018.1475443

[24] Karthik K, Dhanuskodi S, Gobinath C, et al. Fabrication of MgO nanostructures and its efficient photocatalytic, antibacterial and anticancer performance. J Photochem Photobiol B Biol. 2019;190:8–20.

[25] Revathi V, Karthik K. Physico-chemical properties and antibacterial activity of Hexakis (Thiocarbamide) Nickel(II) nitrate single crystal. Chem Data Collect. 2019;21:100229.

[26] Dhanuskodi S. Structural and optical properties of microwave assisted cdo-nio nanocomposite. Aip Conf Proc. 2016;1731:050021.

[27] Mondal S, Bhattacharya SR, Mitra P. Preparation of manganese-doped ZnO thin films and their characterization. Bull Mater Sci. 2013;36:223.

[28] Wood KASung LP, et al. Relating gloss loss to topographical features of a pvdf coating. Technol Res. 2006;3(1):29.

[29] Karthik K, Pushpa S, Madhukara Naik M, et al. Influence of Sn and Mn on structural, optical and magnetic properties of spray pyrolysed CdS thin films. Mater Res Innov. 2019;1–5.

[30] HU, Ugwu EI. Optical Characteristics of Nano crystaline Thermal Annealed Tin Oxide (SO2) Thin Film samples Prepared by Chemical Bath Deposition Technique. Adv Appl Sci Res. 2010;1(3):240. http://www.imedpub.com/articles/optical-characteristics-of-nanocrystaline-thermal-annealed-tin-oxide-so2-thin-film-samples-prepared-by-chemical-bath-deposition-te.pdf

[31] Kim SW, Matusuishi SNomura T. Metallic state in a lime–alumina compound with nanoporous structure. Nano Lett. 2007;7:1138.

[32] Kannan RValanarasu S, et al. Studies on optical and electrical properties of silar-deposited cuo thin films. Mater Res Innov. 2017;21:146–151.

[33] Nagarethinam VSUsharani K, et al. Structural, morphological, optical and electrical properties of spray deposited ternary cdags thin films towards optoelectronic applications. Mater Res Innov. 2018;22:79–84.

[34] Sankarasubramanian NKavitha A, et al. Studies on structural, optical, electrical and morphological properties of licoo2 thin films prepared by sol–gel method. Mater Res Innov. 2019;23:216–221.

[35] ZC, Sung HHChen CY, et al Improvement of the adhesion of the backside Mo electrode in a copper indium gallium selenide solar cell with good electrical properties. Mater Res Innov. 2015;19:S8-512-S8-517.

[36] Serrao FJDharmaprakash SM. Structural, optical and electrical properties of sol–gel prepared ga:zno thin film. Materials Research Innovations. 2016;20:470–474. DOI: 10.1179/1433075X15Y.0000000059

[37] Wang F, Wang YHuang LY, Effect of grain boundaries and grains on electrical properties of fes2 films. Mater Res Innov. 2011;15(6):410–414.

[38] Abdullah A, Abdullah SZAli AMM, Electrical properties of peo–licf3so3–sio2 nanocomposite polymer electrolytes. Mater Res Innov. 2009;13(3):255–258.

[39] Luo YLZhang KP., Electrical response behaviour of doped polyaniline conducting materials induced by thf vapour. Mater Res Innov. 2007;11(3):148–153.

[40] Patel BHLakshminarayana D., Fabrication and electrical characterization of p-znin2se4/n-si heterojunction diode structure. Mater Res Innov. 2016;20(4):285–292.

[41] Pandey KNMathur GN, et al. Revealing the concept if polyarylsilaneimide quasi nano composite formation correlation with macroseopic properties and electrical parameters. Mater Res Innov. 2004;8(2):103–114.